





A model-based motion capture marker location refinement approach using inverse kinematics from dynamic trials

Mark A. Price¹  | Andrew K. LaPrè²  | Russell T. Johnson³  |
Brian R. Umberger⁴  | Frank C. Sup IV¹ 

¹Department of Mechanical and Industrial Engineering, University of Massachusetts, Amherst, Massachusetts

²FTL Labs Corporation, Amherst, Massachusetts

³Department of Kinesiology, University of Massachusetts, Amherst, Massachusetts

⁴School of Kinesiology, University of Michigan, Ann Arbor, Michigan

Correspondence

Mark A. Price, Department of Mechanical and Industrial Engineering, University of Massachusetts, Amherst, MA 01003.
Email: mprice@umass.edu

Funding information

Division of Information and Intelligent Systems, Grant/Award Number: IIS-1526986; National Center for Simulation in Rehabilitation Research, Stanford University, Grant/Award Number: Full Pilot 2014; National Science Foundation, Grant/Award Number: IIS-1526986

Abstract

Marker-based motion capture techniques are commonly used to measure human body kinematics. These techniques require an accurate mapping from physical marker position to model marker position. Traditional methods utilize a manual process to achieve marker positions that result in accurate tracking. In this work, we present an optimization algorithm for model marker placement to minimize marker tracking error during inverse kinematics analysis of dynamic human motion. The algorithm sequentially adjusts model marker locations in 3-D relative to the underlying rigid segment. Inverse kinematics is performed for a dynamic motion capture trial to calculate the tracking error each time a marker position is changed. The increase or decrease of the tracking error determines the search direction and number of increments for each marker coordinate. A final marker placement for the model is reached when the total search interval size for every coordinate falls below a user-defined threshold. Individual marker coordinates can be locked in place to prevent the algorithm from overcorrecting for data artifacts such as soft tissue artifact. This approach was used to refine model marker placements for eight able-bodied subjects performing walking trials at three stride frequencies. Across all subjects and stride frequencies, root mean square (RMS) tracking error decreased by 38.4% and RMS tracking error variance decreased by 53.7% on average. The resulting joint kinematics were in agreement with expected values from the literature. This approach results in realistic kinematics with marker tracking errors well below accepted thresholds while removing variance in the model-building procedure introduced by individual human tendencies.

KEYWORDS

biomechanical optimization, motion capture, subject-specific models

1 | INTRODUCTION

The placement of model markers on musculoskeletal models is an essential task in matching model kinematics to experimental motion capture kinematics. Ideally, model markers and experimental markers should be located in the exact same anatomical location to enable accurate reconstruction of the position of each limb segment captured during

a trial. Realistically, however, model simplifications, limits on motion capture spatial resolution, and soft tissue motion prevent an exact match between the model and the experimental data.

Current best practice places the model markers using averaged marker and segment positions from a person maintaining a static pose to establish an initial set of marker locations.^{1,2} The initial model marker set is commonly placed using photographs of the subject, known anatomical landmarks, and experimental marker data from this static trial. The model segment lengths are scaled by matching the distance between model anatomical landmark markers and experimental anatomical landmark markers from this pose. Model marker positions can then be refined by calculating the model pose for the static trial with inverse kinematics (IK) and adjusting the model marker locations to match the static positions of the experimental markers.

Because experimental markers can move in ways not reproducible by a model due to factors such as soft tissue and clothing motion, marker placement inaccuracies, and musculoskeletal model simplifications, markers cannot be placed in static positions relative to the underlying bone, which exactly match dynamic experimental data. The amount of soft tissue motion typically present during specific experimental tasks has been established by prior works on the subject,^{3,4} and even a perfectly defined model should not produce marker tracking errors smaller than the experimental soft tissue motion. In the case of level walking, root mean square (RMS) marker error has been shown to be on the order of approximately 10 to 18 mm for the thigh and approximately 7 to 14 mm for the shank.⁴ The IK problem is commonly solved using a global optimization method in which model coordinates are calculated to minimize weighted marker and coordinate errors relative to experimental values for each camera frame.⁵ Model markers may then need to be iteratively adjusted to reduce model marker tracking error as well as artifacts in the joint kinematics such as unrealistic magnitudes of hyperextension. This method of model marker placement is typically a manual and iterative procedure. The placement of the marker set is based on the habits and intuition of the person performing the task and, as such, is subject to variability between operators.⁶ This dependence on operator experience and discretion to create accurate models has motivated research to increase model fidelity by algorithmically optimizing model properties and marker positions.⁶⁻¹⁰

Optimization is a common strategy in biomechanics when solving an indeterminate problem in a repeatable way. For example, optimization approaches are used to compute muscle controls,¹¹⁻¹³ model mass properties,¹⁴ mass properties and kinematics from experimental external forces (residual reduction algorithm [RRA]),¹⁵ and model joint properties and kinematics from experimental position data.^{5,16-19} Higher level optimizations can be used to further refine the user-defined conditions for these lower level optimizations. For example, improved kinematic agreement and smaller residual forces have been obtained by optimizing the weights for the kinematic tracking tasks in the RRA.²⁰

With respect to model calibration, bilevel optimization has been used by solving IK for the model and starting marker set using the global optimization method and iteratively adjusting model properties with a higher-level optimization method to minimize IK marker errors.⁹ However, this method requires a large amount of computational power due in part to the use of a particle swarm optimization method at a higher level. A more computationally efficient method has been devised, which combines both optimization levels into a single gradient-based optimization problem.⁷ This was used to refine the joint parameters of a model using dynamic experimental trials.⁸ This method resulted in increased accuracy of prediction of knee contact force during gait and reduced sensitivity of this measure to marker placement. However, this method is subject to the limitations of other gradient-based methods in that it is susceptible to converging to local minima, which is an especially prominent risk in large-scale optimization problems. These methods also carry a risk of overfitting the model parameters to experimental artifacts and knowing which model parameters to optimize and which to hold constant is not a trivial task.^{7,8} Risk of overfitting, and to a lesser degree, vulnerability to local minima, and prohibitive computational expense are the primary disadvantages of previous methods that we attempt to address in this paper.

One potential method for addressing overfitting the model parameters is to limit a refinement algorithm to adjust only the IK tracking marker positions relative to the model anatomy, while determining model segment lengths with a manual approach.¹ Assuming that the physical markers are accurately placed on anatomical landmarks, deriving the musculoskeletal model proportions from the distances between them during static trials could form a more reliable “ground truth” measure than adjusting model proportions to minimize marker tracking error, especially for dynamic trials of walking or range-of-motion exercises that introduce soft-tissue artifact. Algorithmically, refining the tracking marker positions for dynamic trials would create task-specific marker position sets which minimize IK tracking errors without altering the anatomical proportions of the model, reducing the effect of soft-tissue artifact on the model as a whole. Soft tissue artifact would still influence the refined marker set, but the marker positions should roughly correspond to the mean positions relative to the limb segments during the task of interest. This method would remove

human inconsistency from the marker-placement process and potentially improve IK tracking accuracy during dynamic tasks by adjusting marker positions to more closely reflect their actual average positions with soft tissue motion included.

Our goal with this paper is to test the effectiveness of the previously described approach and to provide an open-source model refinement tool, which utilizes it. As such, we developed a marker placement refinement algorithm to interface with the IK tool in OpenSim.²¹ We hypothesize that optimizing IK tracking marker placement on manually scaled models by minimizing IK tracking errors for dynamic trials will reduce human inconsistency from the marker-placement process while avoiding the pitfalls of model overfitting. In this paper, we explain the algorithm in detail and demonstrate its use by refining musculoskeletal models of eight able-bodied human subjects who participated in motion capture gait trials. We compare the marker error metrics and model joint kinematics generated from IK analyses of the refined and manually placed marker sets and examine the trade-off between marker error reduction and computation time. We discuss the contributions and limitations of this approach and identify avenues for future work and conclude with a summary of our findings.

2 | METHODS

2.1 | Model marker placement refinement algorithm

The presented method refines model marker placements by minimizing IK tracking errors for a given experimental task. A well-scaled model and an initial set of model markers are required as input. The iterative marker placement is performed after the model segment lengths and joint positions have been determined and does not make any changes to these parameters. The markers are individually moved relative to their associated model segments until tracking errors are minimized. This approach is constructed as a bilevel optimization problem, where solving the IK problem is the lower-level optimization, the output of which is used to define the objective function in the upper-level marker placement optimization. This upper-level optimization algorithm resembles a pattern search algorithm, which does not require the calculation of a gradient.²² A diagram depicting the information and logic flow of the algorithm is illustrated in Figure 1.

The marker placement algorithm sequentially places model markers in 3-D relative to their assigned rigid segment using the MATLAB interface to the OpenSim API. IK is performed for a dynamic motion capture trial to calculate the tracking error with each marker coordinate modification. The change in the tracking error determines the search direction and size for each coordinate. A final marker placement is reached when the total search interval size for every coordinate is less than a user-defined threshold.

The algorithm works as follows. First, model markers are compiled into a sequential list and then further decomposed into the x, y, and z components of the position vector relative to the segment they are attached to. The dynamic IK solution is found for the initial condition, using marker weights predetermined by the user and which remain constant during the process. The first model marker coordinate is then perturbed by a prescribed search length in the positive direction, and the dynamic IK solution is found and compared with the initial condition. If the objective function has decreased—defined by a summed marker error term and a summed joint kinematic error term when joint kinematics are known—the algorithm will continue to search in that direction. If the objective has increased, the algorithm will search in the opposite direction from the initial condition and perform the same check. Once a search direction has been determined, the algorithm will continue to advance in that direction, checking the IK solution each time. The first iteration that produces an increase in the objective function terminates the search, and the previous value is used. If the initial search direction evaluations both increase the objective, then the initial condition is determined to be optimal, and the search procedure moves to the next marker coordinate. If perturbing the coordinate does not change the objective, the coordinate is determined to have no effect on the IK solution and is not moved.

This procedure continues for every marker coordinate sequentially. Specific marker coordinates can be “locked” from being adjusted by the algorithm as in Andersen et al.⁷ This may be done to minimize overfitting markers with high magnitudes of soft tissue artifact but which can be confidently placed—for example, ASIS markers are located above prominent bony landmarks but are in locations subject to significant skin motion during walking. Locking marker coordinates may also be required to ensure that the optimization solution is sufficiently constrained to be unique and nonarbitrary. Otherwise, it is possible to converge to a solution with very low marker error but with marker positions on the rigid segments unrelated to their experimental positions and physiologically unrealistic model poses.

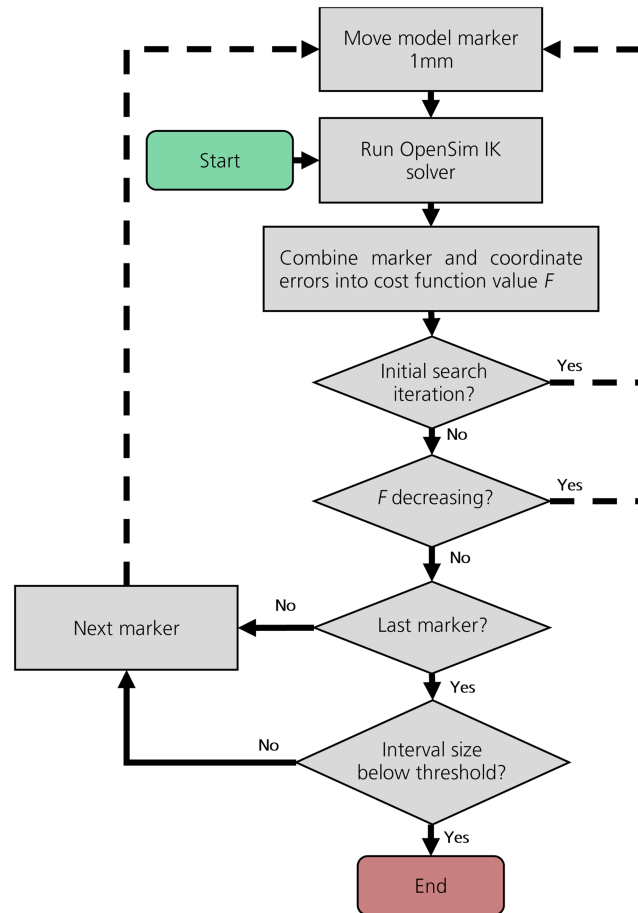


FIGURE 1 Model marker placement refinement algorithm as implemented within OpenSim

The convergence criteria are checked after all variables have been evaluated. Convergence is currently declared if the adjustment magnitude of each marker coordinate for the last adjustment iteration is smaller than some threshold value—the spatial resolution of the motion capture system, for example. If convergence is not determined, the algorithm repeats, starting from the new marker positions. The algorithm outputs a model with the adjusted marker positions if all coordinates satisfy the convergence threshold.

Terms in the objective function other than measures for marker error may be included. Model coordinates with known values in the experimental motion may be considered in the objective function by attempting to minimize the difference between the known value and the value output by IK. This process can also be used to reduce nonphysiological motion artifacts in the solution by explicitly penalizing them in the objective function—for example, severe pelvis tilt in the sagittal plane during able-bodied gait caused by the use of a rigid head-arms-torso segment in the model. The aggressiveness of this reduction can be controlled by weighting it against the marker error penalty. This overlaps with the ability to include experimental model coordinates in the IK lower-level optimization. While acceptable results may be obtained using either approach, the merits of including experimental model coordinate tracking in the marker placement objective versus the IK objective has not yet been investigated.

This algorithm provides a generic method for placing components on a model. As such, it can be extended to adjust other static model location parameters, such as the location and orientation of a joint in a rigid segment. The present work focuses on use of the approach as a marker placement algorithm, but it has also been used to define the equilibrium position of a prosthesis socket relative to the residual tibia in amputee models in LaPrè.²³

2.2 | Test case implementation

To demonstrate this method with a test case, it was used to refine model marker placements for eight able-bodied subjects (four males and four females; age 26 ± 2 years; height 1.74 ± 0.09 m; mass 76.8 ± 14.4 kg) performing level-ground

walking trials at three different stride frequency conditions. Subjects were between the ages of 21 to 40 years and had no history of gait pathologies, injuries, or surgeries within the past year that would affect the way they walked. Subjects were in good general health with no cardiovascular disease, neurological disease, or orthopedic problems that would affect how they walked. Markers were placed on the test subjects by the same researcher across subjects for model scaling and motion tracking. Scaling markers included left and right acromion process, iliac crest, anterior superior iliac spine (ASIS), posterior superior iliac spine (PSIS), greater trochanter, lateral and medial femoral condyles, lateral and medial malleoli, first metatarsal head, fifth metatarsal head, and the tip of the second toe. Tracking markers included acromion processes, iliac crests, ASISs, PSISs, toes, clusters of four markers on the thighs, shank, and clusters of three markers on the heels of the shoes.

Preferred stride frequency (PSF) was determined while subjects walked on a treadmill (Woodway, Waukesha, WI, USA) at a speed of 1.3 m/s. Subjects walked on the treadmill for 10 minutes before calculation of PSF (to allow for warm-up and acclimation to treadmill), then PSF was determined by counting the number of strides the subject took during 60 seconds while walking on the treadmill. Three PSF measurements were taken, and then an average was calculated, this value was used as the subject's PSF. The PSF (0.91 ± 0.03 Hz), 20% slower than PSF (M20: 0.74 ± 0.05 Hz), and 20% faster than PSF (P20: 1.06 ± 0.04 Hz) conditions were all based on the calculated average value.

Kinematic (Qualisys Track Manager, Gothenburg, Sweden; 240 Hz) and kinetic (AMTI, Watertown, MA, USA; 1200 Hz) data were collected simultaneously as subjects stood in a static pose for model scaling purposes. Marker trajectory and ground reaction force data were then collected as subjects walked overground, with the conditions presented in a randomized order. Before each condition, subjects were instructed to practice walking at the target stride frequency for 5 minutes on the treadmill before the overground trials for that condition. While practicing on the treadmill, and for all subsequent overground trials, subjects walked while matching the beat of a digital auditory metronome, set to the targeted stride frequency. Overground walking speed was monitored with timing gates placed 6 m apart along the walkway. Five trials were collected for each condition, and conditions were accepted when the subject walked at the target speed ($\pm 3\%$), stepping to the beat of the metronome, while stepping on three consecutive force plates. Positions of the reflective markers were low-pass filtered using a dual-pass Butterworth filter (6 Hz).

In the IK solution process, more weight was placed on markers that are less susceptible to soft-tissue artifact, such as the rigid clusters, while certain other markers, such as the markers over the greater trochanters, were used for scaling but were not used in IK. A successful experiment trial was defined as one where the subject stepped fully onto the three force platforms in a sequential pattern with alternating feet but without looking down to target the platforms. Walking speed was measured with photogates placed 6 m apart. Five successful trials were recorded per stride frequency, per subject so that within-subject ensemble averages could be calculated.

Models were modified for each subject individually from the “gait2392” model provided by OpenSim as a generic model. The models were scaled, and the initial marker placements were set using the OpenSim scale, and IK tools with motion capture data from the static pose and a single PSF trial for each subject. Segment scales, IK weights, and marker placements were manually and iteratively refined to generate IK solutions of the experimental data in accordance with the guidelines set by the OpenSim user guide (RMS error < 20 mm, maximum error < 40 mm).² A list of markers used in scaling and IK with the corresponding weights is provided in Table 1. This manual model configuration was performed based only on the marker data, with no joint information considered. We acknowledge that including joint angles in the model scaling process may have resulted in more accurately configured models, but we also ensured that the tracking performance of each model was adequate through manual refinement. These models comprise the “Manual” condition. These models were further refined using the marker placement algorithm using a single PSF trial for each subject. The sternum marker and the left and right ASIS markers were used as locked placement “anchor” markers. The objective function consisted of a least squares marker error term as calculated by the OpenSim IK solver² and a pelvis tilt penalty term, both summed across the duration of the trial of the form

$$f = \alpha \sum_{t=0}^N \left[\sum_{i \in \text{markers}} w_i \|\mathbf{x}_i^{\text{exp}}(t) - \mathbf{x}_i(t)\|^2 \right]^2 + \beta \sum_{t=0}^N \theta_p^2(t),$$

where α and β are weighting factors for the marker error and pelvis tilt terms, respectively, $\mathbf{x}_i^{\text{exp}}(t)$ is the experimental position of marker i at time t , $\mathbf{x}_i(t)$ is the corresponding model marker, w_i is the individual marker weight, $\theta_p(t)$ is the pelvis tilt in radians relative to a neutral standing position at time t , and N is the total number of time intervals in the trial. For this experiment, $\alpha/\beta \sim 10^6$. These weights allow the pelvis tilt term to influence the model to walk upright but with marker error dominating the solution. The algorithm was run with a search interval size of 1 mm. The

TABLE 1 List of markers and the model configuration tasks each was used for

Marker Name	Scaling	IK Tracking	IK Weight
Sternum	No	Yes	1
R.Acromium	No	Yes	1
L.Acromium	No	Yes	1
Top.Head	Yes	Yes	1
R.ASIS	Yes	Yes	20
L.ASIS	Yes	Yes	20
R.PSIS	Yes	Yes	10
L.PSIS	Yes	Yes	10
R.Great.Tro	Yes	No	-
L.Great.Tro	Yes	No	-
R.Iliac.Crest	Yes	Yes	1
L.Iliac.Crest	Yes	Yes	1
V.Sacral	Yes	Yes	1
R.Thigh.Upper.Post	No	Yes	10
R.Thigh.Upper.Ant	No	Yes	10
R.Thigh.Lower.Ant	No	Yes	10
R.Thigh.Lower.Post	No	Yes	10
R.Knee.Lat	Yes	Yes	1
R.Knee.Med	No	No	-
R.Shank.Upper.Post	No	Yes	10
R.Shank.Upper.Ant	No	Yes	10
R.Shank.Lower.Ant	No	Yes	10
R.Shank.Lower.Post	No	Yes	10
R.Ankle.Lat	Yes	Yes	1
R.Ankle.Med	No	No	-
R.Heel.Upper	Yes	Yes	1
R.Heel.Med	No	Yes	10
R.Heel.Lat	No	Yes	10
R.Toe.Lat	No	Yes	10
R.Toe.Med	No	Yes	10
R.Toe.Tip	Yes	Yes	1
L.Thigh.Upper.Post	No	Yes	10
L.Thigh.Upper.Ant	No	Yes	10
L.Thigh.Lower.Ant	No	Yes	10
L.Thigh.Lower.Post	No	Yes	10
L.Knee.Lat	Yes	Yes	1
L.Knee.Med	No	No	-
L.Shank.Upper.Post	No	Yes	10
L.Shank.Upper.Ant	No	Yes	10
L.Shank.Lower.Ant	No	Yes	10
L.Shank.Lower.Post	No	Yes	10

(Continues)

TABLE 1 (Continued)

Marker Name	Scaling	IK Tracking	IK Weight
L.Ankle.Lat	Yes	Yes	1
L.Ankle.Med	No	No	-
L.Heel.Upper	Yes	Yes	1
L.Heel.Med	No	Yes	10
L.Heel.Lat	No	Yes	10
L.Toe.Lat	No	Yes	10
L.Toe.Med	No	Yes	10
L.Toe.Tip	Yes	Yes	1
Cervical.Spine	No	Yes	1
Back	No	Yes	1

Note. Tracking weights indicate the amount of influence the corresponding marker has on the inverse kinematics (IK) solution.

convergence criteria (maximum coordinate search distance) were parametrically varied from 1 to 50 mm to identify the point of diminishing returns on model accuracy vs computing cost. The marker placements obtained from one trial were used to calculate IK for the additional trials and stride frequency sets for the corresponding subject. These joint kinematics were compared with able-bodied gait patterns previously established in literature²⁴ to verify that the model kinematics align with expected patterns. RMS and maximum marker error are compared between the manual marker placement and the algorithmic marker placement for the range of convergence thresholds. Average RMS error is defined as RMS marker error averaged across all time points in the gait cycle and across trials. Average maximum marker error is defined as the maximum marker tracking error value for any marker at any point in the gait cycle for each trial, averaged across trials. The marker error and average time to convergence are also compared for the range of convergence thresholds. The computer used to run the algorithm contained a 2.8 GHz Intel Xeon W3530 4-core processor.

The marker placement algorithm has been implemented for OpenSim using the MATLAB scripting interface. MATLAB scripts and example templates, as well as the models and experimental dataset used for this study, can be downloaded from <https://github.com/UMass-OpenSim/opensim-marker-place-toolbox>.

3 | RESULTS

RMS and maximum marker errors for all three stride frequencies across all eight subjects at the 1 mm convergence threshold are reported in Figure 2. On average, RMS errors decreased by 38.4% and maximum errors decreased by 32.1%. Marker error variance across trials was reduced on average by 53.7% (RMS) and 26.2% (maximum error). Marker error variance across trials for each subject individually was reduced on average by 45.7% (RMS) and 9.7% (maximum error). The greatest error reduction in both RMS and maximum error occurred for the PSF trials, in which total RMS marker error was reduced from 11.3 ± 2.4 mm to 6.3 ± 1.0 mm (variance reflects one standard deviation) for a 44.2% mean reduction. Maximum marker error for the PSF condition was reduced from 34.8 ± 7.5 mm to 20.6 ± 3.3 mm for a 40.8% mean reduction. The smallest error reduction percentage occurred for the P20 stride frequency at 34.0% (RMS error) and 21.8% (maximum error).

RMS marker errors for the PSF condition across all trials are plotted for a range of algorithm convergence thresholds with respect to the convergence time in Figure 3. As expected, the shortest convergence time (1685 ± 334 s) and the largest marker error (7.6 ± 1.5 mm) are produced for the most relaxed convergence threshold of 50 mm, and the longest convergence time (11140 ± 5019 s) and smallest marker error (6.3 ± 1.0 mm) are produced at the strictest convergence threshold of 1 mm. A Pareto optimum is found at a convergence threshold of approximately 5 mm with RMS marker error of 6.5 ± 1.0 mm and a convergence time of 3707 ± 997 s. This is about 3% more marker error than the strictest convergence case in 33% of the convergence time on average.

The sagittal plane joint kinematics for the manually placed and the minimum RMS marker error solution are plotted in Figure 4. These data are within one standard deviation of each other on average and qualitatively agree with standard

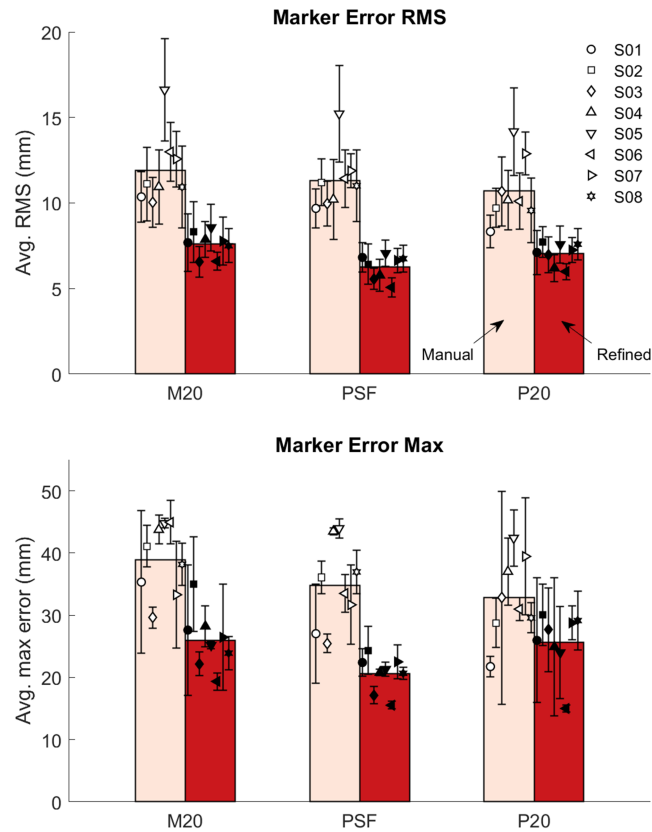


FIGURE 2 Inverse kinematics root mean square (RMS) and maximum marker error for eight able-bodied subjects across three stride frequencies: 20% slower than preferred (M20), preferred (preferred stride frequency [PSF]), and 20% faster than preferred (P20). The bar plot shows the ensemble mean for each condition, and symbols with error bars represent the mean and variance for the individual subjects. Error bars reflect ± 1 SD. Comparison is between marker sets placed and refined using the OpenSim scale tool versus marker sets having undergone the additional refinement provided by the algorithm. Marker error as well as variance decreases when using the algorithm

literature patterns for gait kinematics.²⁴ An offset of approximately 3° extension was observed in the hip angle, and nearly an opposite offset of 3° dorsiflexion was observed in the ankle angle.

4 | DISCUSSION

The goal of this study was to test whether the presented method measurably reduces human operator inconsistency in marker placement across different models while also avoiding overfitting the models to data artifacts. According to the results, tracking error values are more consistent between trials and between models for the set that were algorithmically refined. RMS error values are near to the minimum range of level gait soft tissue motion determined in other studies,⁴ and the joint kinematics closely follow expected behaviors,²⁴ suggesting that if there is some overfitting, the effect is not severe.

IK marker errors were observed to be reduced from that of the manually placed model for every convergence threshold in this study. This included a threshold (50 mm) that allowed convergence after a single pass through each marker coordinate. We expected to reduce marker errors down to approximately 7 mm at minimum given the typical range of soft tissue motion during level walking.⁴ The strictest convergence threshold regularly produced combined RMS marker errors between 5 and 7 mm, which edges the limit of what would be reasonable before indicating an overfitting problem. Marker error reduction was less on average for the non-PSF stride frequencies, which was expected considering each marker set is optimized for a PSF trial. However, RMS marker error was reduced by at least 30% and maximum marker error by at least 20% in all cases. Additionally, the variance in RMS marker error across trials was consistently reduced by using the algorithm for all stride frequencies. These marker error averages are similar to those obtained in previous model refinement studies focusing on data from a single subject⁷⁻⁹ but with less variance across trials despite

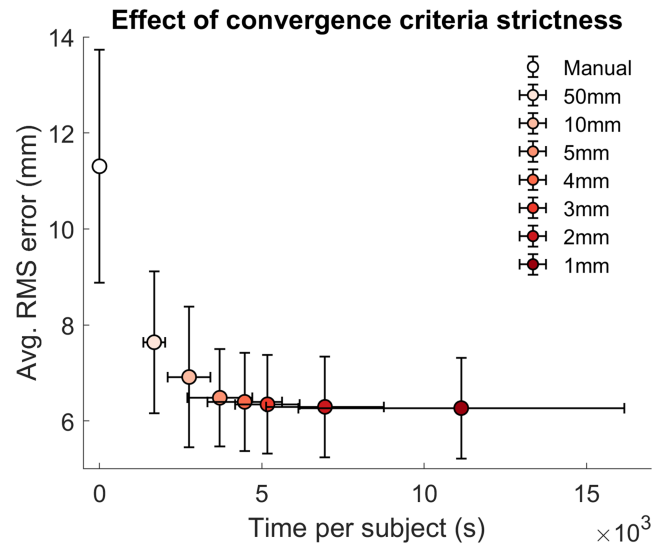


FIGURE 3 Inverse kinematics root mean square (RMS) marker error and time to convergence as a result of changing the convergence threshold value. RMS marker error of the manually placed marker sets is provided for comparison. Pareto optimum near 3 mm search interval size threshold. Error bars reflect ± 1 SD

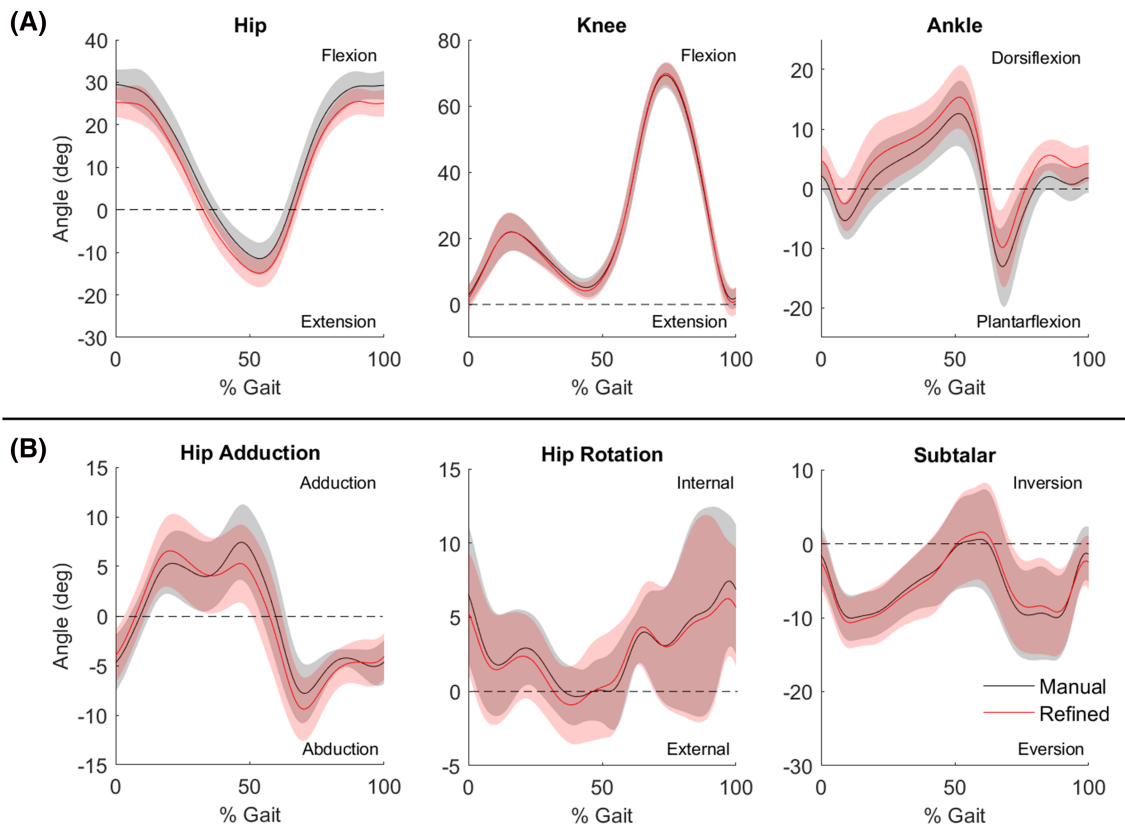


FIGURE 4 Joint kinematics resulting from inverse kinematics solutions of unrefined and refined models. A, Sagittal plane kinematics; B, Kinematics modeled in other anatomical planes. Shaded variance reflects ± 1 SD

the inclusion of multiple subjects. This reduction in variance may be due to the algorithm being constrained to only move the marker positions, producing less error reduction on the trial used for optimization than could be achieved if the model segment parameters were also adjusted. Some model overfitting may be occurring, as indicated by the marginally smaller than expected RMS marker error for the PSF trials. However, the IK tracking being more consistent across trials may also indicate some robustness against model overfitting. Notably, the algorithm strongly reduced the tracking error variance not only across trials for each model but also across the separate models, making the tracking

error mean more consistent between different subjects. This is likely the primary value of the present approach: reducing between-subject variability associated with manual model marker placement and processing.

It was desired to avoid an algorithmic behavior that moved markers far from the positions indicated by photographs of the subjects in search of a theoretical optimum. The maximum distance a lower-limb marker was moved from its original location was 31 mm (thigh cluster, S06) with the typical marker movement being 10 mm averaged across all models. This relatively small distance suggests that this method places markers at physiologically consistent locations when appropriately constrained. Upper limb markers tended to move farther—up to 80 mm in one case (top of head, S06). Because our model used a single rigid segment to represent head, arms, and torso, it was expected that the marker tracking on this segment should be less accurate than on the lower limb segments. These markers were also weighted one order of magnitude less than the marker clusters on the shank and thigh for the formulation of our IK problem, given we were focused on lower limb kinematics during gait. Therefore, large adjustments of torso markers should have minor effects on the IK solution, and we expected larger adjustments of these markers compared with the lower limb markers due to the simplified behavior of the segment they were attached to in our model.

The convergence behavior of the algorithm shows that the variance in time to convergence decreased as the convergence threshold increased, while the variance of the marker error showed the opposite trend. At the 50 mm convergence threshold, almost every marker set converged in one search iteration, resulting in a low time variance but left the variance in marker error near to the variance observed in the manually placed condition. As the threshold tightened, the number of iterations increased by a variable amount, as some marker coordinates often reversed changes made in previous iterations as the rest of the marker set changed. However, the marker errors were reduced more uniformly to a range between about 5 and 7 mm. For this case, a convergence threshold of 5 mm was near the Pareto optimum of diminishing returns between marker error and CPU time per subject. Because the time scale of convergence per subject was on the scale of 10^3 to 10^4 seconds, and the process can run independently for each subject, parallelization of the algorithm should scale efficiently with increasing numbers of CPU cores.

Lacking a “ground truth” measure of the joint angles, it is difficult to judge the accuracy of the algorithm output other than in the context of literature data. Because the kinematics of level gait are well-established, and the manually configured models already agree with the literature,²⁴ the desired outcome is for changes in the refined model kinematics to be minor. Being able to recreate expected gait kinematics may potentially be used as evidence for the reliability of the algorithm when used for experiments that are not already well characterized.

The joint kinematics obtained using the new algorithm showed an offset (3° - 4°) in the hip and ankle angles relative to the manually placed marker set. The data corresponding with the manually placed marker set agree slightly more with literature values of able-bodied gait kinematics,²⁴ with the hip angle ranging from about 30° flexion to 10° extension, whereas the marker placement algorithm tended towards centering the hip angle about zero, depending on the constraints and objectives. The size of this offset increased to shift the hip flexion range from approximately 20° flexion to 20° extension if the ASIS markers were not locked. This resembles the hip angles reported in Lund et al,⁸ which also optimized a model using dynamic trials. Unlocking the ASIS markers caused the algorithmically refined ankle kinematics to agree more closely with the manually placed data, however. Decreasing the weight of the pelvis tilt penalty in the objective function also tended to shift the refined model kinematics to have more hip extension and ankle plantarflexion, as well as increase the variance across subjects. The ankle flexion offset in these alternate conditions was considered less indicative of an overfitting error due to the wider range of variability across subjects and general agreement with the literature. However, the large offsets in the hip kinematics caused by removing algorithm constraints suggest that marker error measures are not sufficient to gauge marker placement accuracy alone, and that use of an algorithmic placement method depends on the judicious use of realistic solution constraints. Such constraints can ensure that a solution is reached within the bounds of uncertainty for expected behavior; however, they can also lead the researcher towards biased results based on a preconceived notion of the “correct” outcome if tuned aggressively.

A concern with any attempt to algorithmically place markers based on minimization of tracking error is overfitting for soft tissue artifact or other experimental artifacts not captured by an ideal model. Aside from marker errors falling below realistic magnitudes, overfitting may be indicated by excessive or noisy joint kinematics. Constraints on the allowed joint behavior may help to combat this—for example, our model does not allow linear translation at the joints. This constraint is an idealization but prevents the marker error minimization from translating the rigid segments to match soft tissue motion in the IK solution. Our algorithm theoretically should place markers near their mean positions relative to the underlying bone during the dynamic task of interest, which may differ from their positions during the static pose. The result is a marker set optimized for tracking the task being analyzed. This marker set may differ for other tasks with different patterns of soft tissue artifact. In this way, we allow the markers to reposition in compensation

for soft tissue artifact while forcing the joints to behave more closely to how we understand them to behave normally. In using the presented method, high-confidence marker positions and joint coordinate patterns should be used to constrain the results to converge to a solution, which agrees with physical reality. Despite adding algorithmic refinement to the process, marker tracking remains somewhat of an art.

Further work on this approach is needed to improve the computational efficiency. The sequential fixed search interval size search method can require hundreds of IK calculations for a single iteration through the entire marker set, and on average took approximately 1 hour per model at the 5 mm convergence threshold. This is significantly slower than the algorithm used to optimize a model from gait trials in Andersen et al⁷—reported as “a few minutes of computational time” at a similar time sample density and using a slower processor than the one used in this study. Our algorithm was designed to ensure that it would not overshoot any minima and converge before refining the marker position below a realistic level of experimental motion capture position accuracy. However, now that an exhaustive search method has been implemented as a baseline point of comparison, a vector gradient and adjustable search interval size as typically used in other gradient-based optimization methods may be appropriate. In addition, other common convergence criteria such as the minimum magnitude of change in output or the minimum vector magnitude of the search interval could be implemented.

A limitation of this approach is that model marker placement is not the only source of error in motion capture analysis. Errors in model scaling are arguably more impactful to the recreated biomechanics than errors in model marker placement. Constraining the optimization to minimize marker error by only adjusting the marker positions may not only make the process more robust to overfitting but also prevents it from rescuing a model that is badly scaled. The degree to which the method can improve a biomechanical analysis in practice is unknown and will likely vary depending on the degree to which the experimental task is already characterized in the literature. This is a compromise approach—it reduces variability between models and improves tracking accuracy as much as the quality of the model scaling and experimental setup will allow while being robust to aggressive model overfitting. The relative importance of removing opportunities for human inconsistency versus constraining avenues for algorithmic overfitting is not concretely defined, and likely varies depending on the experiment being analyzed. Finding ways to improve both through reliably automating both the scaling and marker placement process is an avenue for future work. This work has the potential to be merged with other approaches to algorithmically define joint properties and segment lengths from static and range-of-motion trials to automate a full model configuration process.

5 | CONCLUSION

The presented algorithm has been demonstrated to reduce marker tracking errors and variability in tracking errors across multiple subjects from a manually configured case. Improved accuracy of the model kinematics from this tracking error reduction has not been validated by this study, but it has shown that this method can reproduce kinematic patterns well established in the literature within a one standard deviation margin of error from a traditionally configured model. These results reinforce the primary contributions of this method: introducing repeatability to model configuration tasks and reducing across-subjects variance in IK solutions caused by manual model marker configuration discrepancies.

ACKNOWLEDGMENTS

This work was supported in part by the National Robotics Initiative with a grant from the National Science Foundation (IIS-1526986) and a pilot grant given by the National Center for Simulation in Rehabilitation Research at Stanford University.

ORCID

Mark A. Price  <https://orcid.org/0000-0003-0536-5714>

Andrew K. LaPrè  <https://orcid.org/0000-0001-9474-2539>

Russell T. Johnson  <https://orcid.org/0000-0002-3026-6307>

Brian R. Umberger  <https://orcid.org/0000-0002-5780-2405>

Frank C. Sup IV  <https://orcid.org/0000-0002-6290-9805>

REFERENCES

1. Scaling. OpenSim Documentation. <https://simtk-confluence.stanford.edu:8443/display/OpenSim/Scaling>.

2. Inverse Kinematics. OpenSim Documentation. <https://simtk-confluence.stanford.edu:8443/display/OpenSim/Inverse+Kinematics>.
3. Stagni R, Fantozzi S, Cappello A, Leardini A. Quantification of soft tissue artefact in motion analysis by combining 3D fluoroscopy and stereophotogrammetry: A study on two subjects. *Clinical Biomechanics*. 2005;20(3):320-329. <https://doi.org/10.1016/j.clinbiomech.2004.11.012>
4. Akbarshahi M, Schache AG, Fernandez JW, Baker R, Banks S, Pandy MG. Non-invasive assessment of soft-tissue artifact and its effect on knee joint kinematics during functional activity. *Journal of Biomechanics*. 2010;43(7):1292-1301. <https://doi.org/10.1016/j.jbiomech.2010.01.002>
5. Lu TW, O'Connor JJ. Bone position estimation from skin marker co-ordinates using global optimisation with joint constraints. *Journal of Biomechanics*. 1999;32(2):129-134. [https://doi.org/10.1016/S0021-9290\(98\)00158-4](https://doi.org/10.1016/S0021-9290(98)00158-4)
6. Lund ME, De Zee M, Andersen MS, Rasmussen J. On validation of multibody musculoskeletal models. *Proceedings of the Institution of Mechanical Engineers, Part H: Journal of Engineering in Medicine*. 2012;226(2):82-94. <https://doi.org/10.1177/0954411911431516>
7. Andersen MS, Damsgaard M, MacWilliams B, Rasmussen J. A computationally efficient optimisation-based method for parameter identification of kinematically determinate and over-determinate biomechanical systems. *Computer Methods in Biomechanics and Biomedical Engineering*. 2010;13(2):171-183.
8. Lund ME, Andersen MS, de Zee M, Rasmussen J. Scaling of musculoskeletal models from static and dynamic trials. *International Biomechanics*. 2015;2(1):1-11. <https://doi.org/10.1080/23335432.2014.993706>
9. Reinbolt JA, Schutte JF, Fregly BJ, et al. Determination of patient-specific multi-joint kinematic models through two-level optimization. *Journal of Biomechanics*. 2005;38(3):621-626. <https://doi.org/10.1016/j.jbiomech.2004.03.031>
10. Charlton IW, Tate P, Smyth P, Roren L. Repeatability of an optimised lower body model. *Gait and Posture*. 2004;20(2):213-221. <https://doi.org/10.1016/j.gaitpost.2003.09.004>
11. Davy DT, Audu ML. A dynamic optimization technique for predicting muscle forces in the swing phase of gait. *Journal of Biomechanics*. 1987;20(2):187-201. [https://doi.org/10.1016/0021-9290\(87\)90310-1](https://doi.org/10.1016/0021-9290(87)90310-1)
12. Anderson FC, Pandy MG. Dynamic optimization of human walking. *Journal of Biomechanical Engineering*. 2001;123(5):381-390. <https://doi.org/10.1115/1.1392310>
13. Thelen DG, Anderson FC, Delp SL. Generating dynamic simulations of movement using computed muscle control. *Journal of Biomechanics*. 2003;36(3):321-328. [https://doi.org/10.1016/S0021-9290\(02\)00432-3](https://doi.org/10.1016/S0021-9290(02)00432-3)
14. Vaughan CL, Andrews JG, Hay JG. Selection of body segment parameters by optimization methods. *Journal of Biomechanical Engineering*. 1982;104(1):38-44.
15. Delp SL, Anderson FC, Arnold AS, et al. OpenSim: Open-source software to create and analyze dynamic simulations of movement. *IEEE Transactions on Biomedical Engineering*. 2007;54(11):1940-1950. <https://doi.org/10.1109/TBME.2007.901024>
16. van den Bogert AJ, Smith GD, Nigg BM. In vivo determination of the anatomical axes of the ankle joint complex: an optimization approach. *Journal of Biomechanics*. 1994;27(12):1477-1488. [https://doi.org/10.1016/0021-9290\(94\)90197-X](https://doi.org/10.1016/0021-9290(94)90197-X)
17. Sommer H. A technique for kinematic modeling of anatomical joints. *Journal of Biomechanical Engineering*. 1980;102(4):311-317. <https://doi.org/10.1115/1.3138228>
18. Fregly BJ, Reinbolt JA, Rooney KL, Mitchell KH, Chmielewski TL. Design of patient-specific gait modifications for knee osteoarthritis rehabilitation. *IEEE Transactions on Biomedical Engineering*. 2007;54(9):1687-1695.
19. Reinbolt JA, Haftka RT, Chmielewski TL, Fregly BJ. A computational framework to predict post-treatment outcome for gait-related disorders. *Medical Engineering and Physics*. 2008;30(4):434-443. <https://doi.org/10.1016/j.medengphy.2007.05.005>
20. Samaan MA, Weinhandl JT, Bawab SY, Ringleb SI. Determining residual reduction algorithm kinematic tracking weights for a sidestep cut via numerical optimization. *Computer Methods in Biomechanics and Biomedical Engineering*. 2016;19(16):1721-1729. <https://doi.org/10.1080/10255842.2016.1183123>
21. Seth A, Hicks JL, Uchida TK, et al. OpenSim: simulating musculoskeletal dynamics and neuromuscular control to study human and animal movement. *PLOS Computational Biology*. 2018;14(7):e1006223. <https://doi.org/10.1371/journal.pcbi.1006223>
22. Hooke R, Jeeves TA. "Direct search" solution of numerical and statistical problems. *Journal of the ACM*. 1961;8(2):212-229. <https://doi.org/10.1145/321062.321069>
23. LaPrè AK, Price MA, Wedge RD, Umberger BR, Sup FC. Approach for gait analysis in persons with limb loss including residuum and prosthesis socket dynamics. *International Journal for Numerical Methods in Biomedical Engineering*. 2018;34(4):e2936. <https://doi.org/10.1002/cnm.2936>
24. Winter DA. *Biomechanics and Motor Control of Human Movement*. 4th ed. Hoboken, NJ: John Wiley & Sons; 2009.

How to cite this article: Price MA, LaPrè AK, Johnson RT, Umberger BR, Sup IV FC. A model-based motion capture marker location refinement approach using inverse kinematics from dynamic trials. *Int J Numer Meth Biomed Engng*. 2020;36:e3283. <https://doi.org/10.1002/cnm.3283>